MODELING OF FLEXURAL VIBRATION OF ROTATING SHAFT WITH IN-SPAN DISCRETE EXTERNAL DAMPING

Vikas Rastogi [(a)], Amalendu Mukherjee [(b)], Anirban Dasgupta[(c)]

[(a)] Mechanical Engineering Department
Sant Longowal Institute of Engineering and Technology
Longowal-148106, Punjab, India
[(b)] [(c)] Mechanical Engineering Department
Indian Institute of Technology, Kharagpur, 721302, India

[(a)]rastogivikas@yahoo.com, [(b)]amalendu@mech.iitkgp.ernet.in , [(c)]anir@mech.iitkgp.ernet.in

ABSTRACT
This paper deals with the modeling of one-dimensional continuous systems with in-span discrete external damping. The mathematical formulation for this system is similar to an internally and externally damped rotor driven through a dissipative coupling; however the umbra-Lagrangian density contributed by external damping is different. Using such formulation, the invariance of the umbra-Lagrangian density is obtained through an extension of Noether's theorem. The rotor shaft is modeled as a Rayleigh beam. The dynamic analysis of the rotor shaft is obtained and validated through simulation studies. Results show an interesting phenomenon of limiting behaviour of the rotor shaft with internal damping beyond certain threshold speeds, which are obtained theoretically and affirmed by simulation. The results show that regenerative energy in the rotor shaft due to internal damping is dissipated through the discrete damper as well as the dissipative coupling between drive and the rotor shaft. In such case, the excitation frequency is more, the shaft speed will not increase but the slip between drive and shaft will increase due to loading of drive.

Keywords: Umbra-Lagrangian density, Noether's theorem, Flexural vibration, In-span external damping

1. INTRODUCTION

The methods of Lagrange and Hamilton based on the variational principle on fields are employed to describe continuous systems. There are few direct methods, which approximate the continuous system by considering finite or discrete particles and then examining the changes in the equations describing the motion as the continuous limit is approached. The general relationship between one-parameter continuous symmetries and conserved quantities in field theory has been discussed by Boyer (1967). Cantrijn and Sarlet (1981) had introduced a direct method for associating conserved quantities with each dynamical symmetry group of a Lagrangian system. Some other useful results related with the symmetries aspects of higher Lagrangian and Hamiltonian formulism are discussed in papers of Katzin and Levine (1976) and Damianou and Sophocleous (2004). To extend the scope of Lagrangian-Hamiltonian mechanics, a new proposal of umbra-time was made by Mukherjee (1994). A brief and promising commentary of this kind of extension has been given by Brown (2007). The detailed theory and applications of this extended Lagrangian-Hamiltonian mechanics are presented in various references (Mukherjee et al. 2006, Mukherjee et al. 2007). Recently, Mukherjee et. al.(2009) has applied the extended Lagrangian- Hamiltonian mechanics for one dimensional continuous systems with gyroscopic coupling and non-conservative fields.

The discrete continuous modeling of rotor system was presented by Szoic (2000). In his paper, dynamical investigations of rotor shaft systems are performed by means of the discrete continuous mechanical models. In these systems, rotating cylindrical shaft is represented as continuous systems, whereas bearings are assumed as discrete elements. Krenk (2004) has shown the complex mode analysis of cables and beams problems involving concentrated viscous dampers.

The basic aim of this paper is mainly focused on extending the Lagrangian-Hamiltonian mechanics for discrete-continuous systems. In the extended Lagrangian-Hamiltonian mechanics, umbra-Lagrangian density has been used to describe the motion of the continuous system rather than the umbra-Lagrangian itself. The invariance of umbra-Lagrangian density is obtained through an extension of Noether's theorem over manifolds. The case study considered in this paper shows an interesting phenomenon of limiting behaviour of the rotor shaft with internal damping beyond certain threshold speeds of instability, which are obtained theoretically as well as numerically. The effect of discrete external damping is examined, and entrainment of whirling speeds at natural undamped modes is observed.

2. METHODOLOGY

2.1. Noether's Theorem for Continuous Systems

Constants of motion or conserved quantities can be found for continuous systems by applying Noether's theorem. The Noether's theorem (Noether, 1918) states that under certain conditions there exists a set of integrals of motion or dynamical invariants that characterize a field or a system of fields. In fact, Noether proved her theorem for fields, which is based on invariance of the Lagrangian with respect to a certain group of continuous transformations. Here, the symmetries of the Lagrangian density are applied rather than the Lagrangian itself.

2.2 Extended Formulation of Noether's Theorem for Umbra-Lagrangian Density

Extended formulation of Noether's theorem may be obtained by as the methodology provided in Ref. (Mukherjee et al., 2009). However, some basic concepts are being provided in reference (Mukherjee et al., 2006, 2007, 2009) for ready reference of the readers. The extended Noether's equation may be written as,

$$D_t Z_1 + D_x Z_2 + \lim_{\eta \to t} P_r^3 V_t(\mathcal{L}) = 0 \cdot \tag{1}$$

where,

$$Z_1 = \lim_{\eta \to t} \left[\sum_{i=1}^{2} \xi_i(\eta) \left\{ \frac{\partial \mathcal{L}}{\partial \dot{u}_i(\eta, x)} - \frac{d}{dx}\left(\frac{\partial \mathcal{L}}{\partial \dot{u}_{ix}(\eta, x)} \right) + \frac{d^2}{dx^2}\left(\frac{\partial \mathcal{L}}{\partial \dot{u}_{ixx}(\eta, x)} \right) \right\} \right] \tag{2}$$

$$\begin{aligned} Z_2 = {} & \lim_{\eta \to t} \left[\sum_{i=1}^{2} \left(\xi_i(\eta) \frac{\partial \mathcal{L}}{\partial u_{ix}(\eta, x)} + \xi_i^{/}(\eta) \left(\frac{\partial \mathcal{L}}{\partial u_{ixx}(\eta, x)} \right) - \xi_i(\eta) \frac{d}{dx}\left(\frac{\partial \mathcal{L}}{\partial u_{ixx}(\eta, x)} \right) \right) \right] + \\ & \lim_{\eta \to t} \left[\sum_{i=1}^{2} \left(\dot{\xi}_i(\eta) \frac{\partial \mathcal{L}}{\partial \dot{u}_{ix}(\eta, x)} + \dot{\xi}_i^{/}(\eta) \left(\frac{\partial \mathcal{L}}{\partial \dot{u}_{ixx}(\eta, x)} \right) - \dot{\xi}_i(\eta) \frac{d}{dx}\left(\frac{\partial \mathcal{L}}{\partial \dot{u}_{ixx}(\eta, x)} \right) \right) \right] \end{aligned} \tag{3}$$

Equation (1) is called an extended Noether's field equation for the umbra-Lagrangian. Z_1 may be assumed as local density, Z_2 as current or flux density (often termed as Noether's current density) and the last additional term is called the modulatory convection term, which is the contribution of nonconservative and gyroscopic actions, may be assumed as local rate of production.

3. ANALYSIS OF ROTATING SHAFT WITH IN-SPAN EXTERNAL DAMPING

In this case study, a rotor shaft with internal and in-span discrete external damping driven by a constant speed source through a dissipative coupling is considered as shown in Fig.1. The umbra-Lagrangian of the system is may be written adopting the procedure of Reference (Mukherjee et al., 2009).

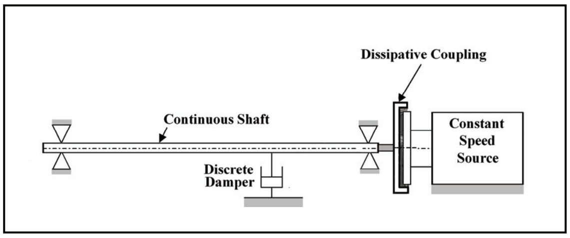

Figure 1: Continuous Shaft with Internal and In-span Concentrated External Damping driven by a Constant Speed Source through Dissipative Coupling.

$$\begin{aligned} \mathcal{L} = {} & \int_{x_0}^{x_1} \left[\begin{aligned} & \sum_{i=1}^{2} \left\{ \begin{aligned} & \frac{1}{2}\rho \left(\frac{\partial u_i(\eta, x)}{\partial \eta} \right)^2 - \frac{1}{2} EI \left(\frac{\partial^2 u_i(\eta, x)}{\partial x^2} \right)^2 \\ & - \frac{1}{2} I_d \left(\frac{\partial^2 u_i(\eta, x)}{\partial \eta \, \partial x} \right)^2 \end{aligned} \right\} \\ & - \mu_i \left\{ \begin{aligned} & \left(\frac{\partial^3 u_1(t, x)}{\partial t \, \partial x^2} + \dot{\theta}(t) \frac{\partial^2 u_2(t, x)}{\partial x^2} \right) \frac{\partial^2 u_1(\eta, x)}{\partial x^2} \\ & + \left(\frac{\partial^3 u_2(t, x)}{\partial t \, \partial x^2} - \dot{\theta}(t) \frac{\partial^2 u_1(t, x)}{\partial x^2} \right) \frac{\partial^2 u_2(\eta, x)}{\partial x^2} \end{aligned} \right\} \end{aligned} \right] dx \\ & \int_{x_0}^{x_1} R_a \delta(x - \lambda)(u_1 \dot{u}_2 - u_2 \dot{u}_1) \, dx \\ & - \left[\begin{aligned} & \mu_i \int_{x_0}^{x_1} \left\{ \frac{\partial^2 u_1(t, x)}{\partial x^2} \frac{\partial^3 u_2(t, x)}{\partial t \, \partial x^2} - \frac{\partial^2 u_2(t, x)}{\partial x^2} \frac{\partial^3 u_1(t, x)}{\partial t \, \partial x^2} \right\} dx \\ & + R_c \left(\dot{\theta}(t) - \Omega \right) \end{aligned} \right] \theta(\eta) \\ & + \frac{1}{2} J \dot{\theta}^2(\eta) \end{aligned} \tag{4}$$

where R_c is the dissipative coupling, R_a is the damping coefficient of in-span external damper, and Ω is the excitation frequency. In Eq. (4), the term contributed by external damping is very significant. For this system with in-span discrete external damping, the term, which needs special consideration, is

$$\int_{0}^{L} R_a \delta(x - \lambda)(u_1 \dot{u}_2 - u_2 \dot{u}_1) \, dx \text{, where } \lambda \in (0, L). \tag{5}$$

In this case, the following form of motion is assumed

$$u_1 = \sum_{n=1}^{\infty} A_n \cos \Omega_n t \sin \frac{n\pi}{L} x \qquad \text{and,}$$

$$u_2 = \sum_{n=1}^{\infty} A_n \sin \Omega_n t \sin \frac{n\pi}{L} x \text{,} \tag{6}$$

where A_n are slowly varying functions of time.

Substitution of Eq. (6) into Eq. (5) yields

$$R_a \left(\Omega_n \sum_{n=1}^{\infty} \sum_{m=1}^{\infty} A_n A_m \sin \frac{n\pi}{L} \lambda \sin \frac{m\pi}{L} \lambda \right), \tag{7}$$

with the assumption that A_n vary slowly with time.

3.1 Extended Noether's theorem for rotating shaft

The modified Noether's rate equation with in span concentrated damping may be expressed as

$$\frac{L}{2}\sum_{n=1}^{\infty} A_n \left[\begin{array}{l} \dot{A}_n + \dfrac{1}{2\rho}\left\{\mu_i \dfrac{n^4\pi^4}{L^4} - \dfrac{\mu_i\, n^4\pi^4}{\Omega_n\, L^4}\dot{\theta}(t)\right\}A_n \\ + \dfrac{R_a}{\rho\, L}\sum\limits_{k=1}^{\infty} A_k \sin\dfrac{n\pi}{L}\lambda\, \sin\dfrac{k\pi}{L}\lambda \end{array}\right] = 0 . \quad (8)$$

Considering independent variations in $A_n + \delta A_n$, the variational equation may be written as (dropping the factor $L/2$)

$$\sum_{n=1}^{n} \delta A_n \left[\begin{array}{l} \dot{A}_n + \dfrac{1}{2\rho}\left\{\mu_i \dfrac{n^4\pi^4}{L^4} - \dfrac{\mu_i\, n^4\pi^4}{\Omega_n\, L^4}\dot{\theta}(t)\right\}A_n \\ + \dfrac{R_a}{\rho\, L}\sum\limits_{k=1}^{\infty} A_k \sin\dfrac{n\pi}{L}\lambda\, \sin\dfrac{k\pi}{L}\lambda \end{array}\right] + \sum_{n=1}^{n} A_n \delta \left[\begin{array}{l} \dot{A}_n + \dfrac{1}{2\rho}\left\{\mu_i \dfrac{n^4\pi^4}{L^4} - \dfrac{\mu_i\, n^4\pi^4}{\Omega_n\, L^4}\dot{\theta}(t)\right\}A_n \\ + \dfrac{R_a}{\rho\, L}\sum\limits_{k=1}^{\infty} A_k \sin\dfrac{n\pi}{L}\lambda\, \sin\dfrac{k\pi}{L}\lambda \end{array}\right] = 0. \quad (9)$$

This is for the symmetry being valid for neighbouring paths, which needs the following conditions to be satisfied

$$\begin{array}{l} \dot{A}_n + \dfrac{1}{2\rho}\left\{\mu_i \dfrac{n^4\pi^4}{L^4} - \dfrac{\mu_i\, n^4\pi^4}{\Omega_n\, L^4}\dot{\theta}(t)\right\}A_n \\ + \dfrac{R_a}{\rho\, L}\sum\limits_{k=1}^{\infty} A_k \sin\dfrac{n\pi}{L}\lambda\, \sin\dfrac{k\pi}{L}\lambda = 0 \end{array} . \quad (10)$$

The condition for entraining the n^{th} mode is $A_n \to$ finite limit and $A_k \to 0$, if $k \neq n$ for $t \to \infty$, obtained as

$$\frac{1}{2\rho}\left\{\mu_i \frac{n^4\pi^4}{L^4} - \frac{\mu_i\, n^4\pi^4}{\Omega_n\, L^4}\dot{\theta}(t)\right\} + \frac{R_a}{\rho L}\sin^2\frac{n\pi}{L}\lambda = 0 , \quad (11)$$

The value of $\dot{\theta}(t)$ will be obtained from Eq. (11) and written as

$$\dot{\theta}(t) = \Omega_n\left[1 + \frac{2R_a L^3}{\mu_i n^4\pi^4}\sin^2\frac{n\pi}{L}\lambda\right]. \quad (12)$$

3.2 Umbra-Hamiltonian density of the system

Umbra-Hamiltonian density for this system may be written as

$$\begin{aligned} \mathcal{H} = \int_{x_0}^{x_1} & \left[\begin{array}{l} \sum\limits_{i=1}^{2}\left\{\begin{array}{l} \dfrac{1}{2\rho}P_i^2(\eta,x) + \dfrac{1}{2}EI\left(\dfrac{\partial^2 u_i(\eta,x)}{\partial x^2}\right)^2 \\ + \dfrac{1}{2}I_d\left(\dfrac{\partial^2 u_i(\eta,x)}{\partial\eta\,\partial x}\right)^2 \end{array}\right\} \\ + \mu_i\left\{\begin{array}{l} \left(\dfrac{\partial^3 u_1(t,x)}{\partial t\,\partial x} + \dot{\theta}(t)\dfrac{\partial^2 u_2(t,x)}{\partial x^2}\right)\dfrac{\partial^2 u_1(\eta,x)}{\partial x^2} \\ + \left(\dfrac{\partial^3 u_2(t,x)}{\partial t\,\partial x} - \dot{\theta}(t)\dfrac{\partial^2 u_1(t,x)}{\partial x^2}\right)\dfrac{\partial^2 u_2(\eta,x)}{\partial x^2} \end{array}\right\} \end{array}\right] dx \\ & + \int_{x_0}^{x_1} R_a(x-\lambda)(u_1\dot{u}_2 - u_2\dot{u}_1)\,dx \\ & + \left[\begin{array}{l} \mu_i \displaystyle\int_{x_0}^{x_1}\left\{\dfrac{\partial^2 u_1(t,x)}{\partial x^2}\dfrac{\partial^3 u_2(t,x)}{\partial t\,\partial x^2} - \dfrac{\partial^2 u_2(t,x)}{\partial x^2}\dfrac{\partial^3 u_1(t,x)}{\partial t\,\partial x^2}\right\}dx \\ + R_c\left(\dot{\theta}(t) - \Omega\right) \end{array}\right]\theta(\eta) \\ & + \frac{1}{2J_d}P_\theta^2, \end{aligned} \quad (13)$$

where $P_i(\eta,x) = \rho\dfrac{\partial u_i(\eta,x)}{\partial\eta}$ and $P_\theta(\eta) = J_d\dot{\theta}(\eta)$.

As discussed in reference (Mukherjee et al., 2009), one has the similar theorems for umbra-Hamiltonian density, expressed as

$$\lim_{\eta\to t}\frac{\partial\mathcal{H}^*}{\partial\eta} = 0 \Rightarrow \frac{d\,\mathcal{H}_i^*}{dt} = -\lim_{\eta\to t}\frac{d\,\mathcal{H}_e^*}{\partial\eta} .$$

Now considering exterior umbra-Hamiltonian density, one may have

$$\begin{aligned} \lim_{\eta\to t}\frac{\partial\mathcal{H}_e}{\partial\eta} = \int_{x_0}^{x_1} & \left[\begin{array}{l} R_a(x-\lambda)(u_1\dot{u}_2 - u_2\dot{u}_1)\,dx \\ + \mu_i\left[\begin{array}{l} \left\{\dfrac{\partial^3 u_1(t,x)}{\partial t\,\partial x^2} + \dot{\theta}(t)\dfrac{\partial^2 u_2(t,x)}{\partial x^2}\right\}\dfrac{\partial^3 u_1(t,x)}{\partial t\,\partial x^2} \\ + \left\{\dfrac{\partial^3 u_2(t,x)}{\partial t\,\partial x^2} - \dot{\theta}(t)\dfrac{\partial^2 u_1(t,x)}{\partial x^2}\right\}\dfrac{\partial^3 u_2(t,x)}{\partial t\,\partial x^2} \end{array}\right] \end{array}\right] dx \\ & + \left[\begin{array}{l} \mu_i \displaystyle\int_{x_0}^{x_1}\left\{\begin{array}{l} \dfrac{\partial^2 u_1(t,x)}{\partial x^2}\dfrac{\partial^3 u_2(t,x)}{\partial t\,\partial x^2} \\ -\dfrac{\partial^2 u_2(t,x)}{\partial x^2}\dfrac{\partial^3 u_1(t,x)}{\partial t\,\partial x^2} \end{array}\right\}dx \\ + R_c\left(\dot{\theta}(t) - \Omega\right) \end{array}\right]\dot{\theta}(t) = 0. \end{aligned} \quad (14)$$

Considering end conditions of continuous shaft as pin-pin, and substituting Eq. (6) in Eq. (14), one obtains the following two terms distinguished as $\{M\}$ and $\{N\}$,

$$\underset{\eta\to t}{Lim}\frac{\partial\mathcal{H}_e}{\partial\eta}=R_a\Omega_n\sum_{n=1}^{\infty}\sum_{m=1}^{\infty}A_nA_m\sin\frac{n\pi}{L}x\sin\frac{m\pi}{L}x$$

$$+\mu_i\frac{L}{2}\left[\begin{array}{l}\sum\limits_{n=1}^{\infty}A_n^2\Omega_n^2\left(\frac{n\pi}{L}\right)^4\\+\dot{\theta}(t)\sum\limits_{n=1}^{\infty}A_n^2\Omega_n\left(\frac{n\pi}{L}\right)^4+\sum\limits_{n=1}^{\infty}\dot{A}_n^2\left(\frac{n\pi}{L}\right)^4\end{array}\right]$$

$$------------Term\{M\}--------$$

$$+\left[\mu_i\left\{\int_0^L\sum_{n=1}^{\infty}A_n^2\Omega_n\sin^2\frac{n\pi x}{L}\left(\frac{n\pi}{L}\right)^4\right\}dx+R_c\left(\dot{\theta}(t)-\Omega\right)\right]\dot{\theta}(t).$$

$$---------------Term\{N\}------------$$

Equating term $\{M\}$ to zero, one obtains

$$\dot{A}_n^2+A_n^2\Omega_n\left[\begin{array}{l}\frac{\mu_i\Omega_n n^4\pi^4}{L^4}-\frac{\mu_i n^4\pi^4}{L^4\Omega_n}\dot{\theta}(t)\\+\frac{2R_a}{L}\sin^2\frac{n\pi}{L}\lambda\end{array}\right]=0\,.$$

Considering independent variations in $A_n+\delta A_n$, the variational equation may be written similar to Eq. (9) after dropping the factor $L/2$. Repeating the same steps from Eq. (10) to (11), one obtains the value of $\dot{\theta}(t)$ as

$$\dot{\theta}(t)=\Omega_n\left[1+\frac{2R_aL^3}{\mu_i n^4\pi^4}\sin^2\frac{n\pi}{L}\lambda\right],$$

which makes the term $\{M\}$ zero and also matches with Eq. (12).

Equating term $\{N\}$ to zero, one obtains

$$\mu_i\sum_{n=1}^{\infty}A_n^2\Omega_n\left(\frac{n\pi}{L}\right)^4\int_0^L\phi_n^2dx+R_c\left(\dot{\theta}(t)-\Omega\right)=0\,. \qquad (10)$$

If the shaft's speed is latched at $\dot{\theta}(t)=\Omega_n\left[1+\frac{2R_aL^3}{\mu_i n^4\pi^4}\sin^2\frac{n\pi}{L}\lambda\right]$, then all the amplitudes go to zero except A_n, thus; the amplitude of this shaft is obtained as

$$A_n=\sqrt{\frac{2R_c\left(\Omega-\underset{n\in I^+}{Min}\,\Omega_n\left[1+\frac{2R_aL^3}{\mu_i n^4\pi^4}\sin^2\frac{n\pi}{L}\lambda\right]\right)}{\mu_i\frac{n^4\pi^4}{L^3}\Omega_n}},$$

or

$$A_n=\sqrt{\frac{2R_c\left(\Omega-\underset{n\in I^+}{Min}\,\Omega_n\left[1+\frac{2R_aL^3}{\mu_i n^4\pi^4}\sin^2\frac{n\pi}{L}\lambda\right]\right)}{\zeta_n\Omega_n}}, \qquad (11)$$

where $\zeta_n=\mu_i\frac{n^4\pi^4}{L^3}$. The next section presents the modeling of rotating shaft with in span concentrated damping with simulation results.

4. Simulation of rotating shaft with in- span discrete external damping

The physical system with in-span discrete external damping driven through dissipative coupling is shown in Fig.1. The boundary conditions of the rotor shaft are taken as pin-pin. The coupling in the system is absolutely flexible in transverse and bending but torsionally rigid. In this analysis, torsional vibration is not considered. The bond graph technique is being used as a modeling tool and bond graph model of the system is created using object-oriented reusable capsules with in-span discrete external damping.

4.1 Simulation results

The bond graph model (Mukherjee et al. 2006, Karnopp et al., 1990) of the rotor shaft with in span concentrated external damping is simulated on SYMBOLS-Shakti (Mukherjee and Samantaray, 2000), in order to visualize the complex modes of the system. The integrated bond graph model with object-oriented sub models (Mukherjee, Karmakar and Samantaray, 2006) of shaft and hub elements is shown in Fig. 2.

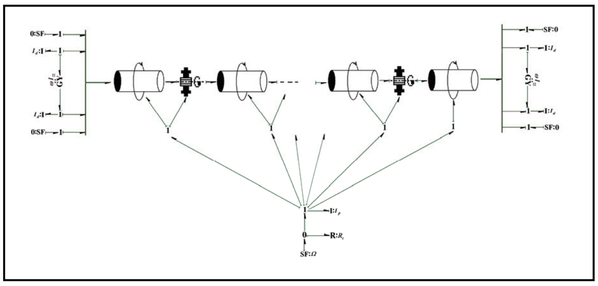

Figure 2: Bond graph Model of Integrated System of Rotor Shaft with Internal and In-span Concentrated External Damping driven by a Constant Speed Source through Dissipative Coupling.

However, the external damping in sub models of shaft has been considered as discrete or finite. In this case, the effects of concentrated damper are closely linked to the complex character of modes. The shaft is rotated by a constant speed source. The simulation rig consists of a hollow rotating shaft with 10 reticules and two ends are well supported on a self-aligning bearing. The dimensional data are as follows: L_{beam}=5 m, R_o=0.02 m, R_i=0.01 m. The material and bearing properties are as follows: E=104.5 e^9, ρ=4420, R_c=0.002, μ_i=2.0 e^{-4}, R_a=0.020 (for Mode 1). The damping coefficient of dissipative coupling is taken as $R_c=0.002$. It has been assumed that in-span discrete damper permits motion to the rotor and at the same time leads to substantial energy dissipation.

Initially, simulation is done for the parameters given in Table-1 with discrete external damping, $R_a=0.020$ and excitation frequency, Ω=5 Hz or 31.41 rad/s. To initiate the simulation, an initial momentum of 0.001 Kg- m^2 was given. This is done to reduce the simulation time. Fig. 3 shows that the trajectories of the rotating shaft reach the limiting orbit.

This is due to the loading of the source. The another feature is that the angular speed of the shaft gets entrained at 22.392 rad/s, the first threshold speed of instability, $\dot{\theta}_{1^{st}\,\mathrm{mode}}$ and matches closely with the calculated value of shaft spinning speed (entrained) $\dot{\theta}(t)$ (Table-1), which is equal to 22.266 rad/s.

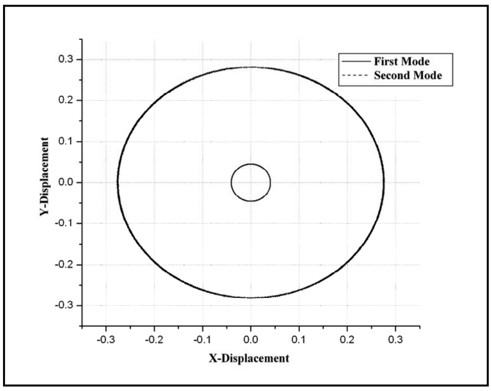

Figure3: Limiting Orbit of Shaft with In-span Concentrated External Damping at First Two Undamped Natural Modes

Table-1: Simulation Parameters

L_{beam}	Length of beam	5 m
N_{elem}	Number of elements	10
E	Modulus of elasticity	104.5 e9 N/m^2
R_i	Internal Diameter	0.01 m
R_o	External Diameter	0.02 m
ρ	Material density	4420 kg/m^3
R_c	Dissipative coupling coefficient	0.002
Ω	Excitation frequency	5 Hz for first mode 30 Hz for second mode
μ_i	Internal Damping Coefficient	1.0 e-4 Ns/m
μ_{ex}	Discrete External Damping Coefficient	0.020 for first mode 6.0 for second mode
$\dot{\theta}(t)$	Shaft Spinning Speed (entrained) Calculated	22.392rad/s, 95.405rad/s, For Mode 1,2, respectively

Table-2: Calculation of Natural Frequency

First mode natural frequency	*3.414 Hz*	Second mode natural frequency	*13.66 Hz*

Now, in span concentrated external damping, R_a of the shaft is increased to 6.0 and excitation frequency, Ω to 30 Hz or 188.327 rad/sec, the next threshold speed of the shaft is obtained. Fig.3 shows the trajectories of the same rotating shaft and angular speed of the shaft gets entrained at 95.490 rad/sec, the second threshold speed of instability, $\dot{\theta}_{2^{nd}\,\mathrm{mode}}$ and matches very close to the calculated value of shaft spinning speed as given in Table-1. The interesting phenomenon observed from this simulation is that the one obtains the natural undamped modes in this case. The result may also be analyzed through FFT analyzer tool as shown in Fig.4, where first two natural frequencies for natural modes are superimposed, which matches exactly with the calculated natural modes as given in Table-2.

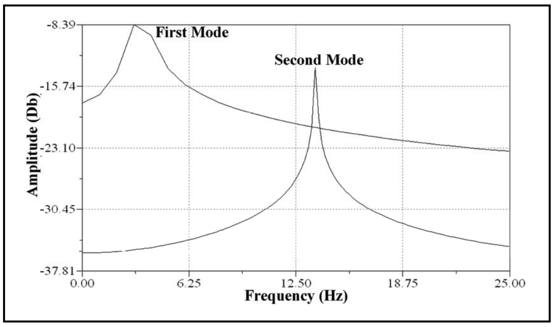

Figure 4: Superimposed Frequency Responses at First Two Undamped Natural Modes.

The results may also be visualized through animation, where two natural modes are shown in Fig. 5(a)- 5(b) through animated frames.

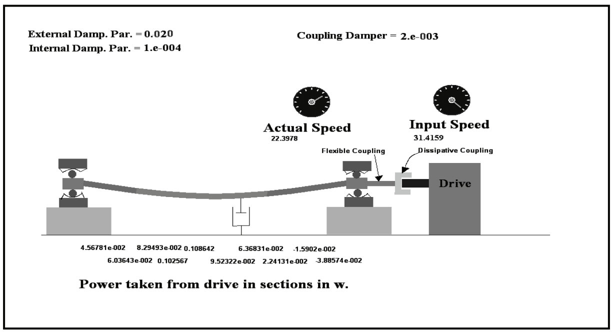

Figure 5(a): First Natural Mode of Rotor Shaft with In span Concentrated External Damping R_a=0.020, μ_i=1e-4, Input Speed=31.41 rad/s, Actual Speed=22.392rad/s.

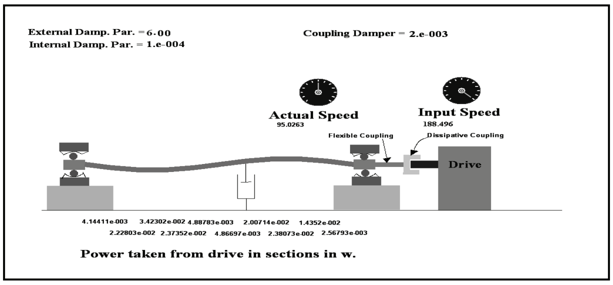

Figure 5(b): Second Natural Mode of Rotor Shaft with In-span Concentrated External Damping R_a=6.00, μ_i=1e-4, Input Speed=188.496 rad/s, Actual Speed=95.490rad/s.

The animation shows that regenerative energy in the shaft due to internal damping is dissipated through the discrete damper and the dissipative coupling between drive and the rotor shaft. If excitation frequency is more, then the shaft speed will not increase but the slip between drive and shaft will increase due to loading of drive.

4. Conclusions

In this paper, interesting case study of a rotor shaft with internal damping and in-span external damping driven through a dissipative coupling has been presented. The dynamic behaviour has been obtained through extended Noether's theorem and umbra-Hamiltonian theoretically as well as numerically. The study has examined the various aspects of limiting dynamics of this rotor and the same results are validated through simulation. Further, the study examined that the regenerative energy in the shaft due to internal damping is dissipated through the in-span damper and the dissipative coupling. Limiting dynamics basically occurred due to the power imported by internal damping from the shaft spin, which is balanced by dissipation of power by in-span external damper, dissipation in the coupling and a part of action of internal damping, acts as a external damping. The animation results of the system have revealed the entrainment of the whirl speed at different natural frequencies.

Nomenclature:

A_n = Amplitude of n^{th} mode of the rotor
EI = Rigidity of the continuous rotor
H^* = Umbra-Hamiltonian of the system
I_d = Rotary inertia of the rotor
I_p = Inertia of the beam through principal axis
L =Lagrangian of the system
L^* = Umbra-Lagrangian of the system
R_c = Damping coefficient of dissipative coupling
R_a = In-span discrete damper
$\boldsymbol{V}$ = Infinitesimal generator of rotational SO (2) group
$\boldsymbol{V}_t$ = Real time component of infinitesimal generator
$\boldsymbol{V}_\eta$ = Umbra time component of infinitesimal generator
a = Cross sectional area of the rotor
n = Mode number
$p(\eta)$ = Umbra-time momentum
$p(t)$ = Real-time momentum
$q(t)$ = Generalized displacement in real time
$q(\eta)$ = Generalized displacement in umbra-time
$\dot{q}(t)$ = Generalized velocity in real time
$\dot{q}(\eta)$ = Generalized velocity in umbra-time
s = Angle or linear variables for rotational transformation or linear transformation.
$x_i(\ )$ = Linear displacements in real time or umbra-time, where $i = 1 \ldots n$
$\dot{x}_i(\ )$ = Linear velocity in real time or umbra-time, where $i = 1 \ldots n$
t = Real-time in s.
Ω = Excitation frequency in rad/s.
Ω_n = Natural frequency of the rotor shaft in rad/s.
η = Umbra-time in s.
ω = constant angular velocity
$\theta(\ )$ = Angular displacement in umbra-time or real time in rad.
$\dot{\theta}(\ )$ = Angular velocity of the shaft in umbra-time or real time in rad/s.
$\mathcal{L}$ = Umbra-Lagrangian density
ρ = Mass density of rotor shaft
μ_a = External damping of the beam
μ_i = Internal damping of the beam
γ^* = Damping ratio
$u_i(t)$ = Real displacement coordinates of beam
$u_i(\eta)$ = Umbra- displacement coordinates of beam
$\mathcal{H}$ = Umbra-Hamiltonian density
$\mathcal{H}_i$, $\mathcal{H}_e$ = Interior and exterior umbra-Hamiltonian density.

Acknowledgements

The authors are thankful to Prof. R. Karmakar, Prof. R. Bhattacharya and Dr. A. K. Samantaray of Dept. of Mech. Engg. IIT, Kharagpur, for their valuable suggestions throughout the course of this study. Moreover, authors would like to thank Mr. Sovendu Banerjee for helping in simulation work.

Reference:

Arnold, V.I., 1974. *Mathematical Methods of Classical Mechanics*, Springer-Verlag, New York–Heidelberg-Berlin, 88.

Boyer, T. H., 1967. Continuous Symmetries and Conserved Currents. *Annals of Physics, 42*(3), 445-466.

Brown, F.T., 2007. Engineering System Dynamics, 2ed, CRC, Taylor & Francis.

Damianou P.A. and C. Sophocleous, 2004. Classification of Noether Symmetries for Lagrangian with Three Degree of Freedom, *Nonlinear Dynamics*, 36, 3.

Hassani, S., 1999. *Mathematical Physics*, Springer-Verlag, New York-Heidelberg-Berlin, 936.

Katzin G.H. and J. Levine, 1976. A Gauge Invariant Formulation of Time-dependent Dynamical Symmetry Mappings and Associated Constants of Motion for Lagrangian Particle Mechanics. *Int. J. Math. Phys*. 17(7), 1345.

Krenk, S., 2004. Complex Modes and Frequencies in Damped structural vibrations, *Journal of Sound and Vibration*, 270, 981-996.

Karnopp, D.C., R.C. Rosenberg, and D.L. Margolis, 1990. *System Dynamics: A Unified Approach*, John-Wiley and Sons Inc., USA .

Mukherjee, A., 1994. Junction Structures of Bondgraph Theory from Analytical Mechanics Viewpoint, *Proc. of CISS-1st Conference of International Simulation Societies*. Zurich, Switzerland, 661.

Mukherjee A. and A. K. Samantaray, 2000. *SYMBOLS-2000 User's Manual*, High-Tech Consultants, STEP Indian Institute of Technology, Kharagpur, India.

Mukherjee, A., V. Rastogi, and A. Dasgupta, 2006. A Methodology for finding Invariants of Motion for Asymmetric Systems with Gauge-transformed Umbra Lagrangian Generated by Bond Graphs, *Simulation*, 82(4), 207-226.

Mukherjee, A. and R. Karmakar, and A. Samantaray, 2006. *Modelling and Simulation of engineering System through Bond Graph*, Narosa publishing House, New Delhi, reprinted by CRC press for North America and by Alpha Science for Europe.

Mukherjee, A., V. Rastogi, and A. Dasgupta, 2007. A Study of a Bi-Symmetric Electro-mechanical System through Umbra Lagrangian Generated by Bond Graphs, and Noether's Theorem, *Simulation*, 83(9), 611-630.

Mukherjee, A., V. Rastogi, and A. Dasgupta, 2009 Extension of Lagrangian-Hamiltonian Mechanics for Continuous Systems-Investigation of Dynamics of a One dimensional internally Damped Rotor driven through a dissipative coupling, *Nonlinear Dynamics*, 58 (1), 107-127.

Szoic, T., 2000. On the discrete Continuous Modelling of Rotor system for the analysis of Coupled Lateral Vibration, *International Journal of Rotating Machinery*, 6 (2), 135-149.

Sarlet W. and F. Cantrijn, 1981. Generalizations of Noether's theorem in Classical Mechanics. *SIAM Rev*., 23(4), 467.

Noether, E., 1918. Invariante Variationsprobleme, *Ges. Wiss. Gottington*. 2, 235.

Olver, P., 1986. *Application of Lie groups to Differential Equations*, Springer-Verlag.

AUTHORS BIOGRAPHY

Vikas Rastogi: He obtained his Master of Technology degree from NIT, Kurukshetra in 1995. In the same year, he joined as a lecturer in Sant Longowal Institute of Engineering & Technology, SLIET, Punjab. He has completed his PhD from IIT, Kharagpur in 2005. He is presently working as an Associate Professor in SLIET, Longowal (Deemed to be University). His research areas are Lagrangian –Hamiltonian mechanics for general class of systems, study of symmetries for discrete and continuous systems, Modeling and Simulation for dynamical systems.

Amalendu Mukherjee: He joined as a lecturer in Mechanical Engineering Department in 1970. In the year 1980, he was awarded Alexander Von Humboldt fellowship for postdoctoral work in Rotor dynamics at Clusthal-Zellerfeld, West Germany. On his return, he undertook the studies on unified approach system modelling through Bond graph theory. He then initiated the creation of family of Software now called SYMBOLS-Shakti for modelling and simulation. SYMBOLS Shakti is being used by several industries, Universities in India and abroad. Presently, he is working in field of Classical mechanics and Study of Symmetries through bond graphs. He is the author of a book as well as Video Course on Bond Graph Modelling of Dynamical Systems.

Anirvan Dasgupta: He received his Ph. D. degree from Indian Institute of Technology, Kanpur. He is presently working as Professor in Mechanical Engineering Department at IIT, Kharagpur. In 2002, he was awarded Alexander Von Humboldt fellowship for postdoctoral work in Germany. His present areas of work are Non-holonomic motion planning, space and under water robot dynamics, and dynamics of continuous systems.